Sulphur-promoted growth of $Mo_6S_2I_8$ nanowires via a metastable $MoI_{2-x}S_x$ intermediate

Anja Pogačnik Krajnc[a, b], Janko Jelenc[a], Luka Pirker[a], Srečo D Škapin[a] and Maja Remškar[a]

[a]Jozef Stefan Institute, Jamova cesta 39, SI-1000, Ljubljana, Slovenia
[b]Faculty of Mathematics and Physics, Jadranska ulica 19, SI-1000 Ljubljana, Slovenia

Supplementary information

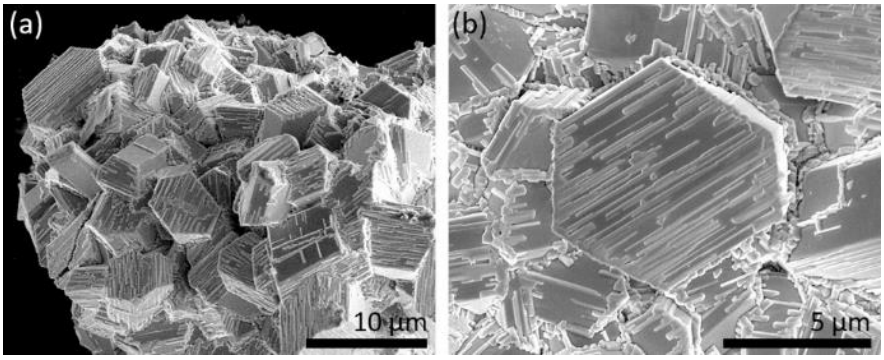

Fig. S1: (a) MoI_2 foil synthesized under conditions comparable to those used for Mo-S-I compound featuring nanowires (NWs). The temperature gradient was set to 1133-1073 K. In this instance, compound did not grow in the shape of nanowires, but the morphology of MoI_2 crystals aligns with those found in the Mo-S-I compound reported in this paper; (b) Six facets of the formed orthorhombic MoI_2 crystal.
EDS (30 kV, 1.6 nA) identifies 31.8 % of Mo and 68.2 % of I. Sulphur was not found, indicating that sulphur did not integrate into the structure during synthesis. The absence of NWs formation implies that the binding of sulphur is essential for effective Mo-S-I NWs synthesis.

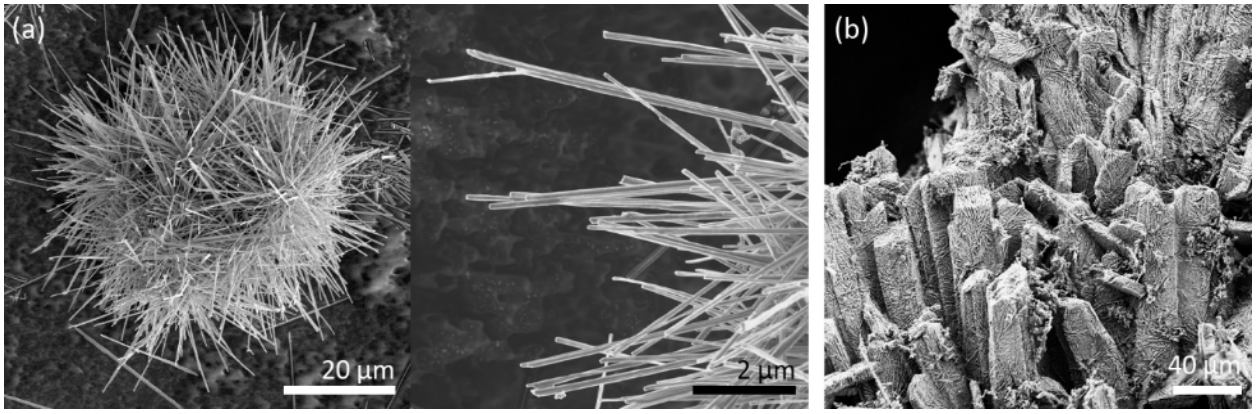

Fig. S2: Scanning electron images of compounds used for analysis of XRD spectra of Mo-S-I: (a) $Mo_6S_2I_8$ nanowires, grow in the shape of a see-urchin in the high-temperature zone of the ampoule. Nanowires are up to 100 µm long and between 100-200 nm long [1-2]. (b) MoI_2 rods synthesized by CVT without the presence of sulphur.

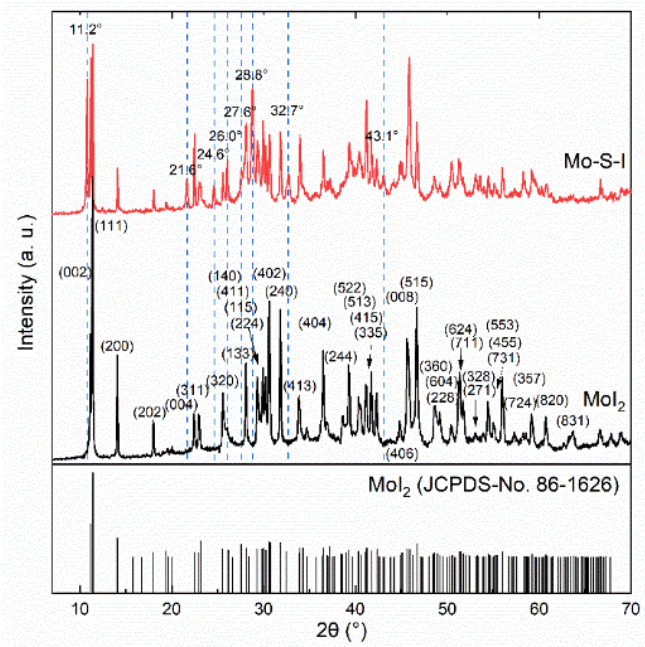

Fig. S3: XRD patterns of Mo-S-I transported material compared to pure MoI_2 and JCPDS card of MoI_2.

Table S1: List of observed XRD peaks and assigned crystallographic planes for peaks measured in MoI_2 rods (Figure S2b) and mixed Mo-S-I peaks. Additional peaks of Mo-S-I are found in the first column:

Additional peaks Mo-S-I compound	Mo-S-I compound	JCPDS-No. 86-1626			
2θ (°)		d (A)	h	k	l
	11.189	7.9015	0	0	2
11.2					
	11.418	7.74329	1	1	1
	14.089	6.28100	2	0	0
	18.027	4.91682	2	0	2
21.6					
	22.487	3.95075	0	0	4
	23.128	3.84266	3	1	1
24.6					
	25.54	3.48407	3	2	0
26.0					
27.6					
	28.112	3.17168	1	3	3
28.8					
	29.290	3.04673	1	4	0
	29.842	2.99164	4	1	1
	29.984	2.97772	1	1	5
	30.253	2.9518	2	2	4
	30.608	2.91843	4	0	2
	31.832	2.80895	2	4	0
32.7					
	33.964	2.63737	4	1	3
	36.520	2.45841	4	0	4
	39.325	2.28930	2	4	4
	40.279	2.23725	5	2	2
	40.385	2.231	5	1	3
	41.118	2.19352	4	1	5
	41.769	2.16082	3	3	5
43.1					
	44.878	2.01806	4	0	6
	45.903	1.97538	0	0	8
	46.711	1.94306	5	1	5
	48.579	1.87263	3	6	0

49.214	1.84995	6	0	4
50.527	1.80490	2	2	8
51.453	1.77458	6	2	4
51.740	1.76541	7	1	1
53.265	1.71839	3	2	8
53.368	1.71533	2	7	1
54.464	1.68338	5	5	3
55.049	1.66685	4	5	5
55.136	1.66443	1	5	7
56.008	1.64056	7	3	1
58.345	1.58030	7	2	4
59.238	1.55858	3	5	7
60.750	1.52337	8	2	0
63.495	1.46395	8	3	1

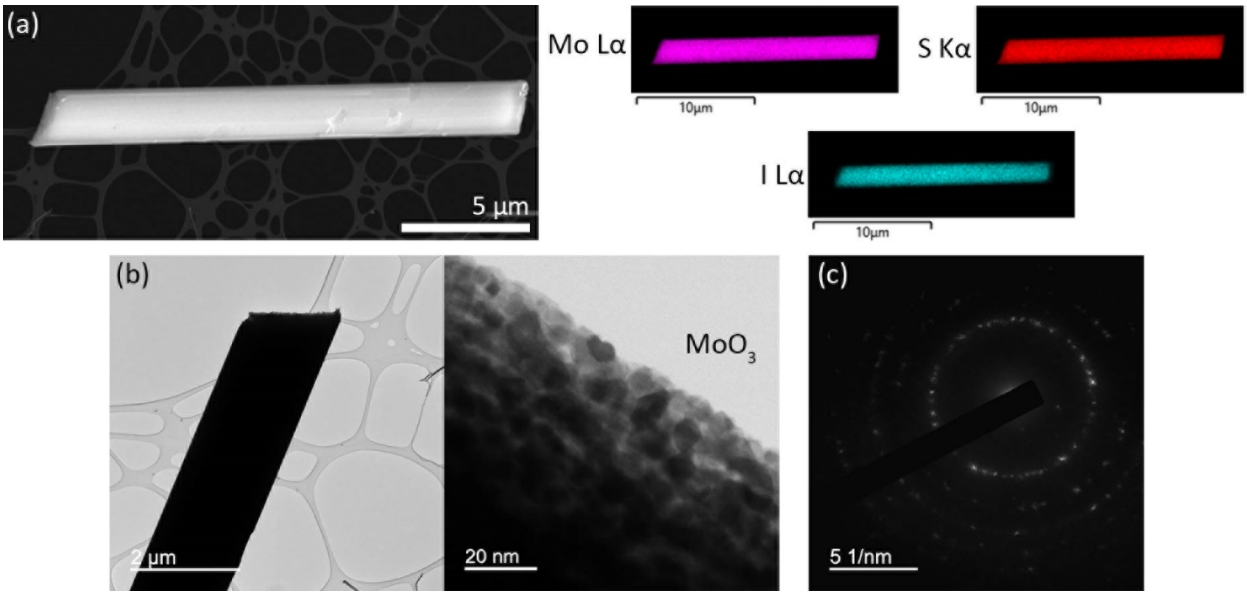

Fig. S4: (a) Partially melted Mo-S-I plate has an even distribution of elements. EDS detects a lower percentage of S on this plate compared to the percentages observed on the nanowires: 1.3 % of S, 33.4 % of Mo and 65.2 % of I; (b) TEM image of the rod that is less stable under electron flux which is noticeable as a decomposition into MoO_3 nanoparticles; (c) SAED pattern of decomposed nanoparticles.

Table S2: Raman mode wavenumbers obtained from the Raman spectra seen in Figure 4c:

	Position of peaks (cm^{-1})																			
532nm rod				95.3			115.9	127.5		137.7			163.4	219.3		286		322		
foil				95.0			117	127.0		138.9			165.9	220.6		285				
633nm rod		78.7		95.0		106.5	116	128		139.5	147.9		164.7	220		284.4		320.5		
foil		76.7		93.9		105.3	115.9	128.1		137.9	147.6		164.5	221		284		320.6		
532nm MoI_2	72.1		86.8		97.7		115.7	129.3	132.2			158.0		217.8	280.8		289.4			

Calibration of work function using HOPG substrate

To determine the work function of Mo-S-I nanowires through contact potential difference (V_{CPD}), we calibrated our AFM tip with the epitaxial gold Au(111) thin film substrate (Phasis Sàrl, Geneva – Switzerland) utilizing the known work function of freshly cleaved highly pyrolytic graphite (HOPG) (SPI Supplies, grade SPI-1): φ_{HOPG} = 4.60 ± 0.05 eV (Fig. S5) [3].

The relation between an AFM tip WF (φ_{TIP}), a sample WF (φ_{SAMPLE}) and the CPD for Omicron VT AFM (V_{CPD}) using Matrix software is defined as $V_{CPD} = (\varphi_{SAMPLE} - \varphi_{TIP})/e$, with e representing the elementary charge. A CPD scan was conducted on the HOPG substrate. The average value of HOPG's CPD was estimated from the line profiles indicated on Fig. S2d: $V_{CPD\ HOPG}$ = 100 mV ± 1 mV. The work function of the tip is then 4.50 eV ± 0.02 eV. An average Au(111)'s CPD was calculated from Fig. S5b: $V_{CPD\ Au}$ = 119 mV ± 1 mV. By employing the work function of tip alongside the typical Au(111)'s CPD value, we successfully calculated the work function of Au(111) :

$$\varphi_{Au} = e\ V_{CPD\ Au} + \varphi_{TIP} = 4.62\ eV \pm 0.02\ eV\ .$$

From this point, we established the work function values of an individual nanowire resting on the Au(111) substrate:

$$\varphi_{NW} = \varphi_{CPD\ NW} + e\ \varphi_{Au}\ .$$

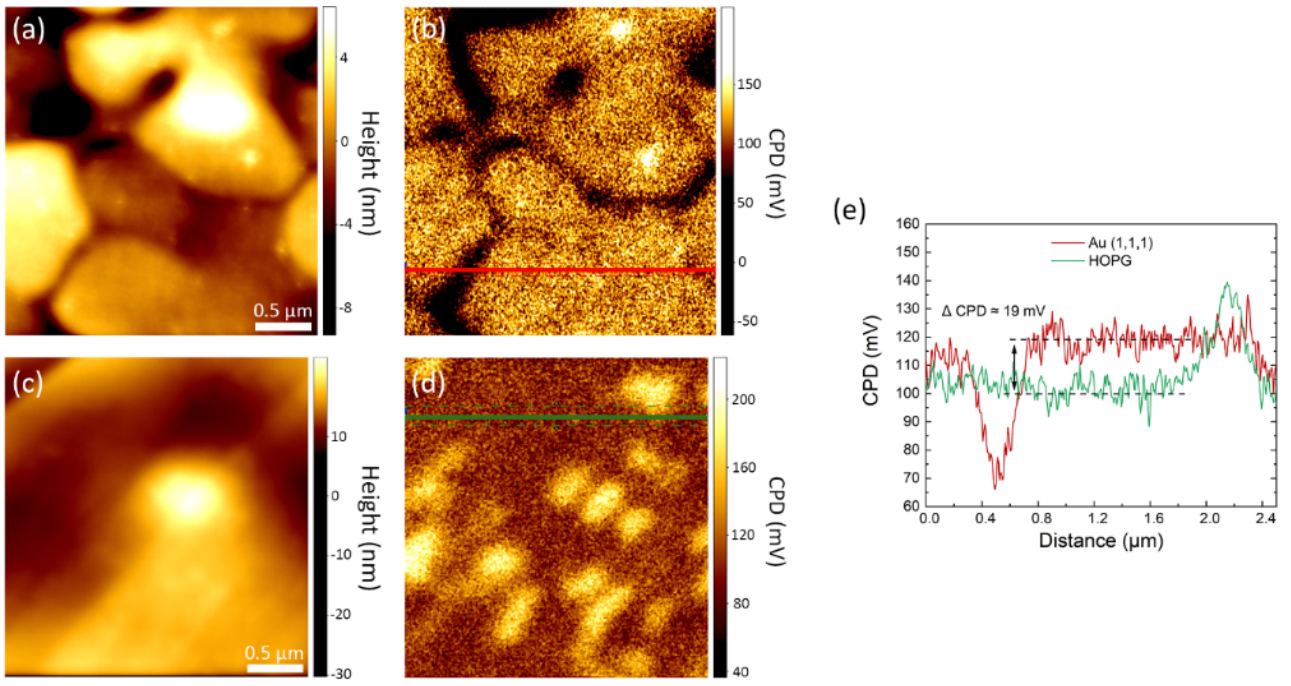

Fig. S5: Topography AFM and corresponding CPD images of (a-b) Au(111) and (c-d) freshly cleaved HOPG substrate; (e) Line profiles of CPD diffrance between substrates was aquired by averaging 10 lines that are marked on the (b) and (d) image. Au(111) has a 19 mV ± 1 mV higher CPD compared to freshly cleaved HOPG.

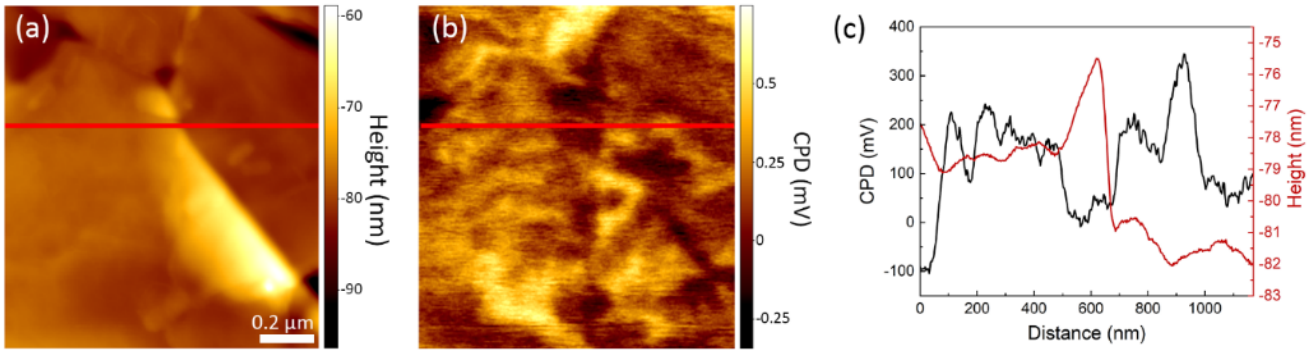

Fig. S6: (a) Topography AFM, (c) CPD image and (b) line profiles obtained on marked region of the backside of Mo-S-I. Kelvin scans show an inhomogenous structure of the back side of Mo-S-I. The size of CPD mostly varies between 100-200 mV. In some places it can also go as high as 300 mV or as low as 10 mV.

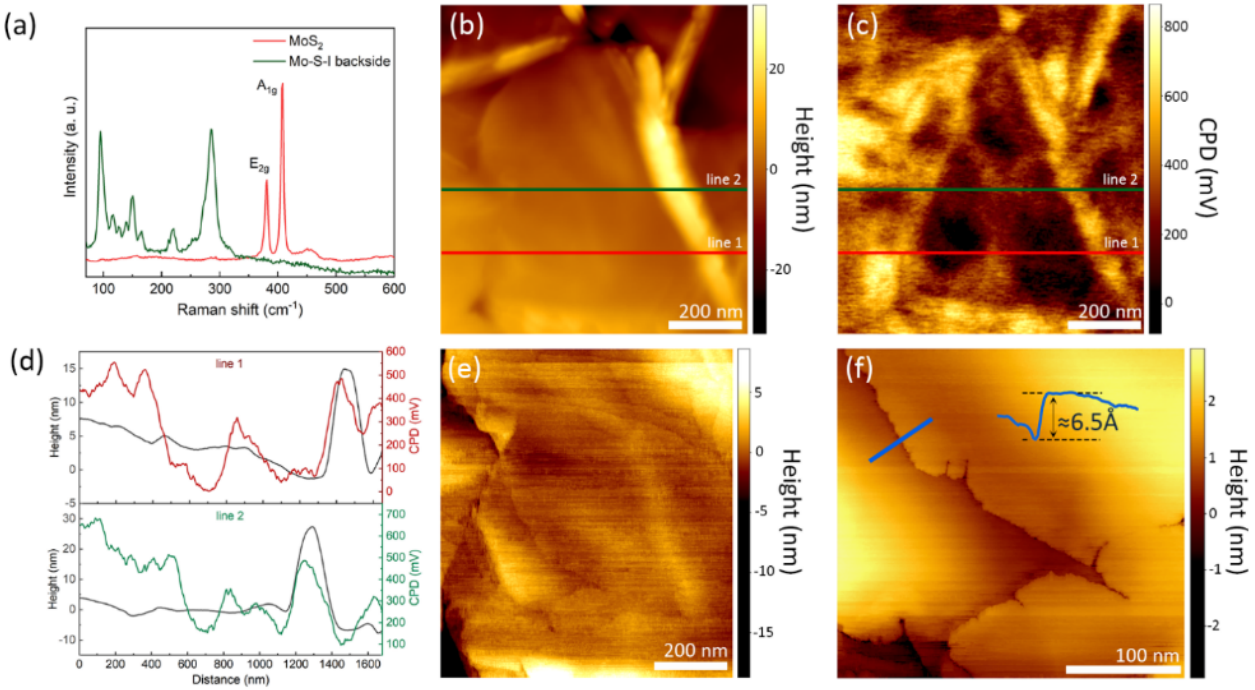

Fig. S7: Triangular shaped MoS_2 flakes growing on the back of Mo-S-I compound (seen in Fig 1d): (a) Raman spectrum on the triangular layered growth differs from the rest of the spectra measured on Mo-S-I. Peak at 379 cm^{-1} ± 0.1 cm^{-1} is assigned as E^1_{2g} (in-plane) mode and 406 cm^{-1} ± 0.1 cm^{-1} is A_{1g} (out-of-plane) MoS_2 mode. Positions of peaks were determined by fitting the data with Lorentzian function; (b) Topography AFM image and (c) simultaneous CPD scan of the area. (d) Topography and CPD line profiles, obtained from the red (line 1) and green line (line 2). A CPD contrast between Mo-S-I and MoS_2 is noticeable with MoS_2 having from 100 and up to 400 mV lower CPD. MoS_2 grows in multiple layers as seen on (d) STM image (3.5 V, 1 nA); (e) The thickness of layer, measured on the left corner of the triangle (≈6.5 Å), is in good agreement with a thickness of MoS_2 monolayer [4], confirming the MoS_2 growth on the backside of Mo-S-I.

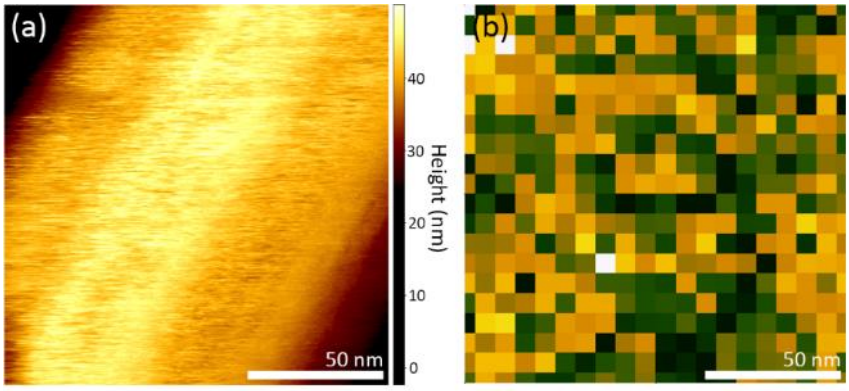

Fig. S8: Mo-S-I nanowire: (a) STM image with corresponding (b) current-imaging-tunnelling spectroscopy (CITS) image (-4.5 V, 0.3 nA).

References

[1] Marko Viršek, Matthias Krause, Andreas Kolitsch, Aleš Mrzel, Ivan Iskra, Srečo D. Škapin, and Maja Remškar. The Transformation Pathways of $Mo_6S_2I_8$ Nanowires into Morphology-Selective MoS_2 Nanostructures, The Journal of Physical Chemistry C 2010 114 (14), 6458-6463 DOI: 10.1021/jp101298g

[2] Marko Viršek, Nikola Novak, Cene Filipič, Peter Kump, Maja Remškar, and Zdravko Kutnjak, *J. Appl. Phys.* 112, 103710 (2012), https://doi.org/10.1063/1.4766451

[3] Wilford N Hansen, Galen J Hansen, Standard reference surfaces for work function measurements in air, Surface Science, Volume 481, Issues 1–3, 2001, Pages 172-184, ISSN 0039-6028, https://doi.org/10.1016/S0039-6028(01)01036-6.

[4] Xiao Li, Hongwei Zhu, Two-dimensional MoS2: Properties, preparation, and applications, Journal of Materiomics, Volume 1, Issue 1, 2015, Pages 33-44, ISSN 2352-8478, https://doi.org/10.1016/j.jmat.2015.03.003.